Dear Author

Here are the proofs of your article.

- You can submit your corrections **online,** via **e-mail** or by **fax**.
- For **online** submission please insert your corrections in the online correction form. Always indicate the line number to which the correction refers.
- You can also insert your corrections in the proof PDF and **email** the annotated PDF.
- For **fax** submission, please ensure that your corrections are clearly legible. Use a fine black pen and write the correction in the margin, not too close to the edge of the page.
- Remember to note the **journal title**, **article number**, and **your name** when sending your response via e-mail or fax.
- **Check** the metadata sheet to make sure that the header information, especially author names and the corresponding affiliations are correctly shown.
- **Check** the questions that may have arisen during copy editing and insert your answers/corrections.
- **Check** that the text is complete and that all figures, tables and their legends are included. Also check the accuracy of special characters, equations, and electronic supplementary material if applicable. If necessary refer to the *Edited manuscript*.
- The publication of inaccurate data such as dosages and units can have serious consequences. Please take particular care that all such details are correct.
- Please **do not** make changes that involve only matters of style. We have generally introduced forms that follow the journal's style.
- Substantial changes in content, e.g., new results, corrected values, title and authorship are not allowed without the approval of the responsible editor. In such a case, please contact the Editorial Office and return his/her consent together with the proof.
- If we do not receive your corrections **within 48 hours**, we will send you a reminder.
- Your article will be published **Online First** approximately one week after receipt of your corrected proofs. This is the **official first publication** citable with the DOI. **Further changes are, therefore, not possible.**
- The **printed version** will follow in a forthcoming issue.

Please note

After online publication, subscribers (personal/institutional) to this journal will have access to the complete article via the DOI using the URL:

`http://dx.doi.org/10.1007/s10846-016-0381-9`

If you would like to know when your article has been published online, take advantage of our free alert service. For registration and further information, go to: http://www.link.springer.com.

Due to the electronic nature of the procedure, the manuscript and the original figures will only be returned to you on special request. When you return your corrections, please inform us, if you would like to have these documents returned.

AUTH

Metadata of the article that will be visualized in OnlineFirst

Please note: Images will appear in color online but will be printed in black and white.

1	Article Title	**A Velocity-Based Dynamic Model and Its Properties for Differential Drive Mobile Robots**	
2	Article Sub-Title		
3	Article Copyright - Year	**Springer Science+Business Media Dordrecht 2016 (This will be the copyright line in the final PDF)**	
4	Journal Name	Journal of Intelligent & Robotic Systems	
5	Corresponding Author	Family Name	**Martins**
6		Particle	
7		Given Name	**Felipe N.**
8		Suffix	
9		Organization	IFES - Federal Institute of Education, Science and Technology of Espírito Santo
10		Division	
11		Address	Serra Campus - Rod. ES-010, km 6,5, Serra, ES, Brazil, 29173-087
12		e-mail	felipe.n.martins@gmail.com
13	Author	Family Name	**Sarcinelli-Filho**
14		Particle	
15		Given Name	**Mário**
16		Suffix	
17		Organization	UFES - Federal University of Espírito Santo
18		Division	Department of Electrical Engineering
19		Address	Av. Fernando Ferrari, 514, Vitória, ES, Brazil, 29075-910
20		e-mail	None
21	Author	Family Name	**Carelli**
22		Particle	
23		Given Name	**Ricardo**
24		Suffix	
25		Organization	INAUT - Institute of Automatics - UNSJ - National University of San Juan
26		Division	
27		Address	Av. San Martin Oeste 1112, San Juan, Argentina, CP 5400
28		e-mail	None
29	Schedule	Received	9 April 2015
30		Revised	
31		Accepted	22 May 2016

AUTH

32	Abstract	An important issue in the field of motion control of wheeled mobile robots is that the design of most controllers is based only on the robot's kinematics. Ho1wever, when high-speed movements and/or heavy load transportation are required, it becomes essential to consider the robot dynamics as well. The control signals generated by most dynamic controllers reported in the literature are torques or voltages for the robot motors, while commercial robots usually accept velocity commands. In this context, we present a velocity-based dynamic model for differential drive mobile robots that also includes the dynamics of the robot actuators. Such model has linear and angular velocities as inputs and has been included in Peter Corke's Robotics Toolbox for MATLAB, therefore it can be easily integrated into simulation systems that have been built for the unicycle kinematics. We demonstrate that the proposed dynamic model has useful mathematical properties and we present an application of such model on the design of an adaptive dynamic controller and the stability analysis of the complete system, while applying the proposed model properties. Finally, we show some simulation and experimental results and discuss the advantages and limitations of the proposed model.
33	Keywords separated by ' - '	Robot dynamics and control - Dynamic modelling - Adaptive control - Mobile robot - 70E60 - 93A30 - 93D05 - 93C40
34	Foot note information	

J Intell Robot Syst
DOI 10.1007/s10846-016-0381-9

A Velocity-Based Dynamic Model and Its Properties for Differential Drive Mobile Robots

Q1 **Felipe N. Martins · Mário Sarcinelli-Filho · Ricardo Carelli**

Received: 9 April 2015 / Accepted: 22 May 2016

Abstract An important issue in the field of motion control of wheeled mobile robots is that the design of most controllers is based only on the robot's kinematics. Ho1wever, when high-speed movements and/or heavy load transportation are required, it becomes essential to consider the robot dynamics as well. The control signals generated by most dynamic controllers reported in the literature are torques or voltages for the robot motors, while commercial robots usually accept velocity commands. In this context, we present a velocity-based dynamic model for differential drive mobile robots that also includes the dynamics of the robot actuators. Such model has linear and angular velocities as inputs and has been included in Peter Corke's Robotics Toolbox for MATLAB, therefore it can be easily integrated into simulation systems that have been built for the unicycle kinematics. We demonstrate that the proposed dynamic model has useful mathematical properties and we present an application of such model on the design of an adaptive dynamic controller and the stability analysis of the complete system, while applying the proposed model properties. Finally, we show some simulation and experimental results and discuss the advantages and limitations of the proposed model.

Keywords Robot dynamics and control · Dynamic modelling · Adaptive control · Mobile robot

Mathematics Subject Classification (2010) 70E60 · 93A30 · 93D05 · 93C40

F. N. Martins (✉)
Q2 IFES - Federal Institute of Education, Science and Technology of Espírito Santo, Serra Campus - Rod. ES-010, km 6,5, Serra, ES, Brazil 29173-087
Q3 e-mail: felipe.n.martins@gmail.com

M. Sarcinelli-Filho
Department of Electrical Engineering, UFES - Federal University of Espírito Santo, Av. Fernando Ferrari, 514, Vitória, ES, Brazil 29075-910

R. Carelli
INAUT - Institute of Automatics - UNSJ - National University of San Juan, Av. San Martin Oeste 1112, San Juan, Argentina, CP 5400

1 Introduction

Most mobile robots are wheel-based structures because of their efficiency and simple mechanical implementation [28]. A very common configuration for mobile robots is the differential drive, which has two independently driven wheels in the rear (or front) and one or more unpowered wheels to balance the structure. Due to their good mobility and simple configuration, differential drive robots have been used in various applications, such as surveillance [3], floor cleaning [24], industrial load transportation [30], autonomous wheelchairs [1], and others.

Considering differential drive mobile robots, an important issue is that the design of most of its motion controllers is based only on the robot's kinematic model. The main reasons for that are: (a) the dynamic model is more complicated than the kinematic one and its precise determination depends on the knowledge of several parameters associated with the vehicle and its actuators (like mass, moment of inertia etc.); and (b) mobile robots frequently have low-level velocity control loops for their motors, which take a desired angular velocity as input and stabilize the motor angular velocity at this value [22].

However, because the robot's low-level velocity control loops do not guarantee perfect velocity tracking, when high-speed movements and/or heavy load transportation are required, it becomes essential to consider the robot dynamics as well, as we also have shown in our previous work [21]. Thus, some motion controllers that compensate for the robot dynamics have been proposed in the literature. As an example, in [11] a combined kinematic/torque control law with a robust-adaptive controller based on neural networks is proposed to deal with disturbances and non-modeled dynamics. Notice that the control commands they used were torques. Another example is the adaptive fuzzy logic-based controller presented in [7]. Their dynamic model includes the actuator dynamics, and the commands generated by the controller are voltages for the robot motors. Other examples of controllers that deal with the unicycle dynamics were presented in [10, 16, 23, 27, 32].

The control signals generated by most dynamic controllers reported in the literature are torques or voltages for the robot motors (as in the above-mentioned papers), while commercial robots usually receive velocity commands, like the Pioneer robots from Adept Mobile Robots, the Khepera robots from K-Team Corporation, and the robuLAB-10 from Robosoft Inc. Following this idea, in [2] a switching controller with on-line learning and hierarchical architecture has been proposed, investigating Neural Network-based methodologies to compensate the effects of non-modeled phenomena. Neural Networks (NN) were used for identification and control, and the control signals were linear and angular velocities. However, the authors reported that real-time implementation of their solution requires a high-performance computer architecture based on a multi-processor system. On the other hand, a dynamic model using linear and angular velocities as inputs has been proposed in [8], along with the design of multi-robot controller. One advantage of such a model is that its parameters are directly related to the robot physical parameters.

To reduce performance degradation in applications in which the robot dynamic parameters may vary (such as load transportation) or when the knowledge of the dynamic parameters is limited, we have proposed an adaptive controller in [21]. There, we have used the dynamic model proposed in [8], but we have divided it in two parts, allowing the design of independent controllers for the robot kinematics and dynamics.

A similar idea was used in the following works, which have also used a dynamic model that has linear and angular velocities as inputs. An adaptive sliding-mode dynamic controller to implement a trajectory-tracking mission was presented in [5]. It proposes a kinematic controller working with an adaptive sliding-mode dynamic controller that makes the real velocity of the wheeled mobile robot reach the desired velocity commands. In turn, in [9] a landmark-based navigation system for robotic wheelchairs is proposed and an adaptive controller considering its dynamic model is developed. An approach to adaptive trajectory tracking of mobile robots is presented in [25], that presents an inverse nonlinear controller combined with an adaptive NN with sliding mode control using an on-line learning algorithm. The adaptive NN acts as a compensator for a controller to improve system performance when it is affected by variations in its structure. Finally, [31] deals with the Nonlinear Model Predictive Control of an agricultural robot to precisely follow a trajectory operating in row cultures in order to perform high precision drop-on-demand application of herbicide.

The above-mentioned works applied a dynamic model that has linear and angular velocities as inputs, which illustrates the interest on such kind of dynamic model. In such context, in this paper we extend our previous work [21] that dealt with a velocity-based dynamic model. The main contributions of the present paper are the proposal of a new approach to represent the dynamics of differential drive mobile robots and the study of its mathematical properties, which are useful on the design of controllers that compensate for the robot dynamics and on the system stability analysis. As in [21], the dynamic model presented here includes the dynamics of the robot actuators and has linear and angular velocities as inputs, which makes its integration into existing simulation models straightforward. We apply the proposed model and some of its properties on the design of an adaptive dynamic compensation controller, with a robust updating law, and present the stability analysis of the whole system as an application example. Several simulation and some experimental results are presented. A comparison of the performance of the system with and without the dynamic compensation controller is also shown. Finally, we discuss the advantages and limitations of the proposed model and present our conclusions.

2 Dynamic Model

The dynamic model for the differential drive mobile robot proposed in [8] is now reviewed. For convenience, we first present its equations again. Then, the dynamic model is written in such a way that it becomes similar to the classical dynamic equation based on torques. Figure 1 depicts a differential drive mobile robot with the variables of interest. There, u and ω are, respectively, the linear and angular velocities, G is the center of mass, h is the point of interest (whose position should be controlled) with

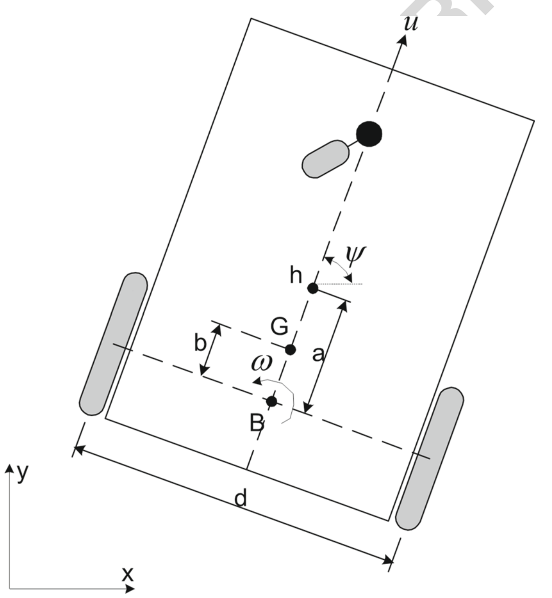

Fig. 1 The differential drive mobile robot

coordinates x and y in the XY plane, ψ is the robot orientation, a is the distance from the point of interest to the point in the middle of the virtual axle that links the traction wheels (point B), b is the distance between points G and B, and d is the distance between the points of contact of the traction wheels to the floor.

In the model, $\boldsymbol{\theta} = [\theta_1, ..., \theta_6]^T$ is the vector of identified parameters and $\boldsymbol{\delta} = [\delta_x \quad \delta_y \quad 0 \quad \delta_u \quad \delta_\omega]^T$ is the vector of parametric uncertainties associated to the mobile robot. The complete mathematical model is written as [8]

$$\begin{bmatrix} \dot{x} \\ \dot{y} \\ \dot{\psi} \\ \dot{u} \\ \dot{\omega} \end{bmatrix} = \begin{bmatrix} u\cos\psi - a\omega\sin\psi \\ u\sin\psi + a\omega\cos\psi \\ \omega \\ \frac{\theta_3}{\theta_1}\omega^2 - \frac{\theta_4}{\theta_1}u \\ -\frac{\theta_5}{\theta_2}u\omega - \frac{\theta_6}{\theta_2}\omega \end{bmatrix} + \begin{bmatrix} 0 & 0 \\ 0 & 0 \\ 0 & 0 \\ \frac{1}{\theta_1} & 0 \\ 0 & \frac{1}{\theta_2} \end{bmatrix} \begin{bmatrix} u_{ref} \\ \omega_{ref} \end{bmatrix} + \begin{bmatrix} \delta_x \\ \delta_y \\ 0 \\ \delta_u \\ \delta_\omega \end{bmatrix}.$$

The parameters included in the vector $\boldsymbol{\theta}$ are functions of some physical parameters of the robot, such as its mass m, its moment of inertia I_z at G, the electrical resistance R_a of its motors, the electromotive constant k_b of its motors, the constant of torque k_a of its motors, the coefficient of friction B_e, the moment of inertia I_e of each group rotor-reduction gear-wheel, the radius r of the wheels, and the distances b and d (see Fig. 1). It is assumed that the robot servos have PD controllers to control the velocities of each motor, with proportional gains $k_{PT} > 0$ and $k_{PR} > 0$, and derivative gains $k_{DT} \geq 0$ and $k_{DR} \geq 0$. It is also assumed that the motors associated to both driven wheels have the same characteristics, and that their inductances are neglectable. The equations describing the parameters θ_i are

$$\theta_1 = \left[\frac{R_a}{k_a}\left(mr^2 + 2I_e\right) + 2rk_{DT}\right]\frac{1}{(2rk_{PT})}[s],$$

$$\theta_2 = \left[\frac{R_a}{k_a}\left(I_e d^2 + 2r^2\left(I_z + mb^2\right)\right) + 2rdk_{DR}\right] \times \frac{1}{(2rdk_{PR})}[s],$$

$$\theta_3 = \frac{R_a}{k_a}\frac{mbr}{2k_{PT}}[sm/rad^2],$$

$$\theta_4 = \frac{R_a}{k_a}\left(\frac{k_a k_b}{R_a} + B_e\right)\frac{1}{r k_{PT}} + 1,$$

$$\theta_5 = \frac{R_a}{k_a}\frac{mbr}{dk_{PR}}[s/m], \text{ and}$$

$$\theta_6 = \frac{R_a}{k_a}\left(\frac{k_a k_b}{R_a} + B_e\right)\frac{d}{2r k_{PR}} + 1.$$

It should be noticed that $\theta_i > 0$ for $i = 1, 2, 4, 6$. The parameters θ_3 and θ_5 can be negative and will be null if, and only if, the center of mass G is exactly in the center of the virtual axle, i.e. $b = 0$.

The above model is split into kinematic and dynamic parts. The kinematic model is

$$\begin{bmatrix} \dot{x} \\ \dot{y} \\ \dot{\psi} \end{bmatrix} = \begin{bmatrix} \cos\psi & -a\sin\psi \\ \sin\psi & a\cos\psi \\ 0 & 1 \end{bmatrix}\begin{bmatrix} u \\ \omega \end{bmatrix} + \begin{bmatrix} \delta_x \\ \delta_y \\ 0 \end{bmatrix}, \quad (1)$$

whereas the dynamic model is

$$\begin{bmatrix} \dot{u} \\ \dot{\omega} \end{bmatrix} = \begin{bmatrix} \frac{\theta_3}{\theta_1}\omega^2 - \frac{\theta_4}{\theta_1}u \\ -\frac{\theta_5}{\theta_2}u\omega - \frac{\theta_6}{\theta_2}\omega \end{bmatrix} + \begin{bmatrix} \frac{1}{\theta_1} & 0 \\ 0 & \frac{1}{\theta_2} \end{bmatrix}\begin{bmatrix} u_{ref} \\ \omega_{ref} \end{bmatrix} + \begin{bmatrix} \delta_u \\ \delta_\omega \end{bmatrix}. \quad (2)$$

Now, we are going to present our proposal for representing the dynamic model. By rearranging the terms, Eq. 2 can be written as

$$\begin{bmatrix} -\theta_1 & 0 \\ 0 & -\theta_2 \end{bmatrix}\begin{bmatrix} \delta_u \\ \delta_\omega \end{bmatrix} + \begin{bmatrix} \theta_1 & 0 \\ 0 & \theta_2 \end{bmatrix}\begin{bmatrix} \dot{u} \\ \dot{\omega} \end{bmatrix} + \begin{bmatrix} \theta_4 & -\theta_3\omega \\ \theta_5\omega & \theta_6 \end{bmatrix}\begin{bmatrix} u \\ \omega \end{bmatrix}$$

$$= \begin{bmatrix} 1 & 0 \\ 0 & 1 \end{bmatrix}\begin{bmatrix} u_{ref} \\ \omega_{ref} \end{bmatrix},$$

or, in a compact form, as

$$\boldsymbol{\Delta} + \mathbf{H}'\dot{\mathbf{v}} + \mathbf{c}(\mathbf{v})\mathbf{v} = \mathbf{v_r}, \quad (3)$$

where $\mathbf{v_r} = [u_{ref} \quad \omega_{ref}]^T$ is the vector of reference velocities, $\mathbf{v} = [u \quad \omega]^T$ is the vector containing the actual robot velocities, and the matrices $\mathbf{H}'$ and $\mathbf{c}(\mathbf{v})$, and the vector $\boldsymbol{\Delta}$ are given by

$$\mathbf{H}' = \begin{bmatrix} \theta_1 & 0 \\ 0 & \theta_2 \end{bmatrix}, \quad \mathbf{c}(\mathbf{v}) = \begin{bmatrix} \theta_4 & -\theta_3\omega \\ \theta_5\omega & \theta_6 \end{bmatrix} \quad \text{and}$$

$$\boldsymbol{\Delta} = \begin{bmatrix} -\theta_1 & 0 \\ 0 & -\theta_2 \end{bmatrix}\begin{bmatrix} \delta_u \\ \delta_\omega \end{bmatrix}.$$

Let us rewrite $\mathbf{c}(\mathbf{v})$ by adding and subtracting the term $i\theta_3 u$ to its fourth element (where $i = 1$ rad^2/s), such that

$$\mathbf{c}(\mathbf{v}) = \begin{bmatrix} \theta_4 & -\theta_3\omega \\ \theta_5\omega & \theta_6 + (i\theta_3 - i\theta_3)u \end{bmatrix}, \quad (4)$$

so that the term $\mathbf{c}(\mathbf{v})\mathbf{v}$ can be written as

$$\begin{bmatrix} 0 & -\theta_3\omega \\ \theta_3\omega & 0 \end{bmatrix}\begin{bmatrix} iu \\ \omega \end{bmatrix} + \begin{bmatrix} \theta_4 & 0 \\ 0 & \theta_6 + (\theta_5 - i\theta_3)u \end{bmatrix}\begin{bmatrix} u \\ \omega \end{bmatrix}. \quad (5)$$

The role of the term $i = 1$ rad^2/s is to make the units consistent to allow us to split $\mathbf{c}(\mathbf{v})$ into two matrices, while keeping the numerical values unchanged. Now, let us define $\mathbf{v}' = [iu \quad \omega]^T$ as the vector of modified velocities, so that

$$\mathbf{v}' = \begin{bmatrix} i & 0 \\ 0 & 1 \end{bmatrix}\begin{bmatrix} u \\ \omega \end{bmatrix}.$$

The terms in the vector of modified velocities are numerically equal to the terms in the vector of actual velocities $\mathbf{v}$, only its dimensions are different. By rewriting the model equation, the following matrices are defined:

$$\mathbf{H} = \begin{bmatrix} \theta_1/i & 0 \\ 0 & \theta_2 \end{bmatrix}, \quad \mathbf{F}(\mathbf{v}') = \begin{bmatrix} \theta_4/i & 0 \\ 0 & \theta_6 + (\theta_5/i - \theta_3)iu \end{bmatrix}$$

and

$$\mathbf{C}(\mathbf{v}') = \begin{bmatrix} 0 & -\theta_3\omega \\ \theta_3\omega & 0 \end{bmatrix}.$$

Finally, we propose the dynamic model of a differential-drive mobile robot to be represented by

$$\boldsymbol{\Delta} + \mathbf{H}\dot{\mathbf{v}}' + \mathbf{C}(\mathbf{v}')\mathbf{v}' + \mathbf{F}(\mathbf{v}')\mathbf{v}' = \mathbf{v_r}. \quad (6)$$

Though written in a different way, the model proposed here is mathematically equivalent to the one proposed in [8], where simulation and experimental results were presented to validate it. The main advantage of the model presented here is that it is written in such a way that it becomes possible to use its mathematical properties in the design and stability analysis of dynamic controllers. Such properties are studied and discussed in the following Section.

3 Dynamic Parameters and Model Properties

Before analyzing the properties of the dynamic model, it is important to verify that none of its parameters θ_1 to θ_6 can be written as a linear combination of the others, otherwise it would be possible to write the dynamic model with a smaller number of parameters. Some physical variables have influence on more than one parameter θ, therefore the linear independence between $\theta_1..\theta_6$ is not straightforwardly seen. This issue was not discussed in previous papers, so we have applied the following method to verify the linear independence of parameters $\boldsymbol{\theta}$: using the equations that define the dynamic parameters (presented in Section 2), we have obtained K sets of parameters calculated with randomly generated values of the physical variables (R_a, I_e, B_e, m, r etc.). The results were used to build the following matrix:

$$\begin{bmatrix} \theta_1(1) & \theta_2(1) & \theta_3(1) & \theta_4(1) & \theta_5(1) & \theta_6(1) \\ \theta_1(2) & \theta_2(2) & \theta_3(2) & \theta_4(2) & \theta_5(2) & \theta_6(2) \\ \theta_1(3) & \theta_2(3) & \theta_3(3) & \theta_4(3) & \theta_5(3) & \theta_6(3) \\ \vdots & \vdots & \vdots & \vdots & \vdots & \vdots \\ \theta_1(K) & \theta_2(K) & \theta_3(K) & \theta_4(K) & \theta_5(K) & \theta_6(K) \end{bmatrix}.$$

This matrix has 6 columns and K lines, where K is the number of random sets of parameters. It was verified that its rank is equal to 6, which indicates that it has six independent columns, i.e. all parameters are linearly independent. In an attempt to avoid a false indication of independence between the parameters due to numerical error, each column of the matrix was normalized by dividing its values by the maximum value of that column. Before calculating the rank of the matrix, all values were truncated so that they had a fixed number of decimal digits. This procedure was repeated several times for $K = 1,000$ and $K = 5,000$. For truncation of 4, 3, and 2 decimal digits, the resulting matrix rank was equal to six in all cases, indicating that the dynamic parameters $\boldsymbol{\theta}$ are, indeed, linearly independent. This indicates that the dynamic model of the differential drive mobile robot cannot be written with less than six parameters.

3.1 Model Properties

First, it is interesting to notice that the dynamic model considers that the robot's center of mass G can be located anywhere along the line that crosses the center of the structure, as illustrated in Fig. 1. This means that the formulation of the proposed dynamic model is adequate for robots that have a symmetrical weight distribution between their left and right sides. Because most differential drive robots have an approximately symmetrical weight distribution (with each motor and wheel on either left or right sides), we claim that this assumption does not introduce significant modeling errors on most cases.

Now, let us analyze the mathematical properties of the dynamic model. First, recall that $\theta_i > 0$ for $i = 1, 2, 4, 6$. By observing that $\mathbf{H}$ is a diagonal square matrix formed by θ_1 and θ_2, one can conclude that $\mathbf{H}$ is symmetric and positive definite, and its inverse exists and is also positive definite. Moreover, $\mathbf{H}$ is constant if there is no change on the physical parameters of the robot (i.e., if there is no change on the robot's mass, moment of inertia etc.), and does not depend on the robot position if it navigates on a horizontal plane.

$\mathbf{F}(\mathbf{v}')$ is also a diagonal square matrix formed by θ_4 and $\theta_6 + (\theta_5/i - \theta_3)iu$. If we assume that $\theta_6 > -(\theta_5/i - \theta_3)iu$, we can conclude that $\mathbf{F}(\mathbf{v}')$ is symmetric and positive definite. Additionally, $\mathbf{F}(\mathbf{v}')$ can be considered constant if $\theta_6 \gg |(\theta_5/i - \theta_3)iu|$ and there is no change on the physical parameters of the robot. In Section 3.2 we show that the conditions of $\theta_6 > -(\theta_5/i - \theta_3)iu$ and $\theta_6 \gg |(\theta_5/i - \theta_3)iu|$ were verified via experimental tests for five different types of robots whose parameters were identified.

$\mathbf{C}(\mathbf{v}')$ is a square matrix formed by $\theta_3\omega$ and $-\theta_3\omega$, whose transpose is also its negative. Therefore, $\mathbf{C}(\mathbf{v}')$ is skew symmetric.

Finally, the following theorem states the passivity property of the dynamic model (6).

Theorem 1 *Considering $\boldsymbol{\Delta} = \mathbf{0}$ and $\theta_6 > -(\theta_5/i - \theta_3)iu$, and assuming that $\mathbf{v_r} \in L_{2e}$ and $\mathbf{v}' \in L_{2e}$, the mapping $\mathbf{v_r} \rightarrow \mathbf{v}'$ of the dynamic model*

$$\mathbf{H}\dot{\mathbf{v}}' + \mathbf{C}(\mathbf{v}')\mathbf{v}' + \mathbf{F}(\mathbf{v}')\mathbf{v}' = \mathbf{v_r}$$

is strictly output passive.

Proof According to [26], an operator $P : L_{2e} \rightarrow L_{2e}$ is strictly output passive if, and only if, there are constants $\delta \in \mathbb{R}$ and $\beta \in \mathbb{R}$ so that

$$< Px, x > \geq \beta + \delta \|Px\|^2_{2,T} \quad \forall x \in L_{2e},$$

where $< \cdot, \cdot >$ represents the internal product. To show that the mapping $\mathbf{v_r} \rightarrow \mathbf{v}'$ is strictly output passive, let us consider the positive function $V = \frac{1}{2}\mathbf{v}'^{\mathbf{T}}\mathbf{H}\mathbf{v}'$ and its first time derivative $\dot{V} = \mathbf{v}'^{\mathbf{T}}\mathbf{H}\dot{\mathbf{v}}'$, where property 4 is applied. Using Eq. 6 and applying properties 3 and 5, $\dot{V}$ can be written as

$$\dot{V} = \mathbf{v}'^{\mathbf{T}}(\mathbf{v_r} - \mathbf{C}\mathbf{v}' - \mathbf{F}\mathbf{v}') = \mathbf{v}'^{\mathbf{T}}\mathbf{v_r} - \mathbf{v}'^{\mathbf{T}}\mathbf{F}\mathbf{v}'. \quad (7)$$

By integrating Eq. 7 one gets

$$\int_0^T \dot{V} dt = \int_0^T \mathbf{v}'^{\mathbf{T}} \mathbf{v_r} dt - \int_0^T \mathbf{v}'^{\mathbf{T}} \mathbf{F} \mathbf{v}' dt,$$

which can be written as

$$V(T) - V(0) = \int_0^T \mathbf{v}'^{\mathbf{T}} \mathbf{v_r} dt - \int_0^T \mathbf{v}'^{\mathbf{T}} \mathbf{F} \mathbf{v}' dt. \quad (8)$$

By neglecting the positive term V(T), it follows that

$$-V(0) \leq \int_0^T \mathbf{v}'^{\mathbf{T}} \mathbf{v_r} dt - \inf(\lambda_{min}(\mathbf{F})) \int_0^T \|\mathbf{v}'\|^2 dt,$$

or

$$\int_0^T \mathbf{v}'^{\mathbf{T}} \mathbf{v_r} dt \geq -V(0) + \inf(\lambda_{min}(\mathbf{F})) \|\mathbf{v}'\|^2_{2,T}.$$

Assuming that $\mathbf{v_r} \in L_{2e}$ and $\mathbf{v}' \in L_{2e}$, the prior equation can be written as

$$< \mathbf{v}', \mathbf{v_r} > \geq -V(0) + \inf(\lambda_{min}(\mathbf{F})) \|\mathbf{v}'\|^2_{2,T}, \quad (9)$$

where $\inf(\lambda_{min}(\cdot))$ represents the smallest eigenvalue of a matrix. Given that $\theta_6 > -(\theta_5/i - \theta_3)iu$, one can see that $\mathbf{F} > \mathbf{0}$. Therefore, based on Eq. 9, one can conclude that the mapping $\mathbf{v_r} \rightarrow \mathbf{v}'$ is strictly output passive. □

To sum up, the mathematical properties of the dynamic model (6) are:

1. The matrix $\mathbf{H}$ is symmetric and positive definite, or $\mathbf{H} = \mathbf{H}^T > 0$;
2. The inverse of $\mathbf{H}$ exists and is also positive definite, or $\exists\ \mathbf{H}^{-1} > 0$;
3. The matrix $\mathbf{F}(\mathbf{v}')$ is symmetric and positive definite, or $\mathbf{F}(\mathbf{v}') = \mathbf{F}^T > 0$, if $\theta_6 > -(\theta_5/i - \theta_3)iu$;
4. The matrix $\mathbf{H}$ is constant if there is no change on the physical parameters of the robot;
5. The matrix $\mathbf{C}(\mathbf{v}')$ is skew symmetric;
6. The matrix $\mathbf{F}(\mathbf{v}')$ can be considered constant if $\theta_6 \gg |(\theta_5/i - \theta_3)iu|$ and there is no change on the physical parameters of the robot;
7. The mapping $\mathbf{v_r} \rightarrow \mathbf{v}'$ is strictly output passive if $\theta_6 > -(\theta_5/i - \theta_3)iu$ and $\boldsymbol{\Delta} = \mathbf{0}$.

3.2 Identified Parameters

In order to verify the assumptions that $\theta_6 \gg |(\theta_5/i - \theta_3)iu|$ and $\theta_6 > -(\theta_5/i - \theta_3)iu$, we have analyzed the dynamic parameters of five differential drive robots, all obtained via an identification procedure. The description of the parameter identification procedure is out of the scope of this paper, but the reader is referred to [8] and [17] for detailed information.

We consider the parameters of the following robots: a Pioneer 3-DX with no extra equipment ($P3$), a Pioneer 3-DX with a LASER scanner and omnidirectional camera ($P3_{laser}$), a robotic wheelchair while carrying a 55 kg person (RW_{55}), a robotic wheelchair while carrying a 125 kg person (RW_{125}), and a Khepera III ($K3$), whose parameters were originally presented in [17]. The Khepera III robot weighs 690 g, has a diameter of 13 cm and is 7 cm high. By its turn, the Pioneer robots weigh about 9 kg, are 44 cm long, 38 cm wide and 22 cm tall (without the LASER scanner). The LASER scanner weighs about 50 % of the original robot weight, which produces an important change in the mass and moment of inertia of the structure. Finally, the robotic wheelchair presents an even greater difference in dynamics because of its own weight (about 70 kg) and the weight of the person that it is carrying. The dynamic parameters for the above mentioned robots are presented in Table 1.

The value of u is limited to 0.5 m/s for the Khepera III robots, to 1.2 m/s for the Pioneer robots, and to 1.5 m/s for the robotic wheelchair. Therefore, using the values presented in Table 1 one can verify that the conditions of $\theta_6 > -(\theta_5/i - \theta_3)iu$ and $\theta_6 \gg |(\theta_5/i - \theta_3)iu|$ are valid for all sets of identified parameters. Therefore, the dynamic model of the above-mentioned robots can be represented as in Eq. 6, with properties 1–7 valid.

4 Application Example: Controller Design

To illustrate the usefulness of the proposed dynamic model and its properties, let us show the design of an adaptive dynamic compensation controller, with

Table 1 Identified dynamic parameters

	$P3$	$P3_{laser}$	RW_{55}	RW_{125}	$KIII$
$\theta_1[s]$	0.5338	0.2604	0.3759	0.4263	0.0228
$\theta_2[s]$	0.2168	0.2509	0.0188	0.0289	0.0568
$\theta_3[sm/rad^2]$	−0.0134	−0.0005	0.0128	0.0058	−0.0001
θ_4	0.9560	0.9965	1.0027	0.9883	1.0030
$\theta_5[s/m]$	−0.0843	0.0026	−0.0015	0.0134	0.0732
θ_6	1.0590	1.0768	0.9808	0.9931	0.9981

stability analysis of the whole control system. The controller design is split in two parts, as in [21]. The first part is based on the inverse kinematics and the second one compensates for the robot dynamics. The application of the proposed model and its properties is shown on the second part.

The control structure is shown in Fig. 2, where blocks **K**, **D** and **R** represent the Kinematic controller, the Dynamic compensation controller, and the Robot, respectively. Figure 2 shows that the Kinematic controller receives the desired values of position $\mathbf{h_d} = [x_d\ y_d]^T$ and velocity $\dot{\mathbf{h}}_\mathbf{d}$ from the trajectory planner (which is not considered in this work). Then, based on those values and on the actual robot position $\mathbf{h} = [x\ y]^T$ and orientation ψ, the Kinematic controller calculates the desired robot velocities $\mathbf{v_d} = [u_d \quad \omega_d]^T$. The desired velocities $\mathbf{v_d}$ and the actual robot velocities $\mathbf{v} = [u \quad \omega]^T$ are fed into the Dynamic controller. Such controller uses those values and the estimates of the robot parameters $\boldsymbol{\theta}$ to generate the actual velocity commands $\mathbf{v_r} = [u_r \quad \omega_r]^T$ that are sent as references to the robot internal controller.

4.1 Kinematic Controller

We use the same kinematic controller that we have presented in [21]. It is a trajectory tracking controller based on the inverse kinematics of the robot. We repeat the controller equation here for convenience. Considering only the position of the point of interest $\mathbf{h} = [x\ y]^T$, the kinematic control law here adopted is

$$\begin{bmatrix} u_d \\ \omega_d \end{bmatrix} = \begin{bmatrix} \cos\psi & \sin\psi \\ -\frac{1}{a} sin\psi & \frac{1}{a}\cos\psi \end{bmatrix} \begin{bmatrix} \dot{x}_d + l_x \tanh\left(\frac{k_x}{l_x}\tilde{x}\right) \\ \dot{y}_d + l_y \tanh\left(\frac{k_y}{l_y}\tilde{y}\right) \end{bmatrix}, \tag{10}$$

for which $\mathbf{v_d} = [u_d \quad \omega_d]^T$ is the vector of desired velocities given by the kinematic controller; $\mathbf{h} = [x\ y]^T$ and $\mathbf{h_d} = [x_d\ y_d]^T$ are the vectors of actual and desired coordinates of the point of interest h, respectively; $\tilde{\mathbf{h}} = [\tilde{x} \quad \tilde{y}]^T$ is the vector of position errors given by $\mathbf{h_d} - \mathbf{h}$; $k_x > 0$ and $k_y > 0$ are the controller gains; $l_x, l_y \in \mathbb{R}$ are saturation constants; and $a > 0$. The tanh terms are included to limit the values of the desired velocities $\mathbf{v_d}$ to avoid saturation of the robot actuators in case the position errors $\tilde{\mathbf{h}}$ are too big, considering $\dot{\mathbf{h}}_\mathbf{d}$ is appropriately bounded.

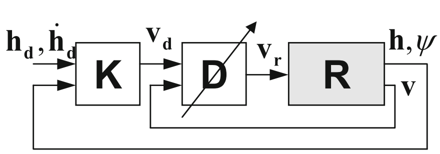

Fig. 2 Structure of the control system

The system characterized so far has a globally asymptotically stable equilibrium at the origin, which means that the position errors $\tilde{x}(t) \to 0$ and $\tilde{y}(t) \to 0$ as $t \to \infty$. The reader should refer to [21] for details on the development and stability analysis of the kinematic controller.

4.2 Adaptive Dynamic Compensation Controller

Now, the use of the proposed dynamic model and its properties is illustrated via the design of an adaptive dynamic compensation controller. It receives the desired velocities $\mathbf{v_d}$ from the kinematic controller and generates a pair of linear and angular velocity references $\mathbf{v_r}$ for the robot servos, as shown in Fig. 2. First, let us define the vector of modified velocities $\mathbf{v}'_\mathbf{d}$ as

$$\mathbf{v}'_\mathbf{d} = \begin{bmatrix} u'_d \\ \omega_d \end{bmatrix} = \begin{bmatrix} i & 0 \\ 0 & 1 \end{bmatrix} \begin{bmatrix} u_d \\ \omega_d \end{bmatrix},$$

and the vector of velocity errors is given by $\tilde{\mathbf{v}}' = \mathbf{v}'_\mathbf{d} - \mathbf{v}'$.

To design the dynamic controller, Eq. 6 is written in its linear parametrization form, as

$$\mathbf{v_r} = \mathbf{G}'\boldsymbol{\theta} = \begin{bmatrix} \dot{u} & 0 & -\omega^2 & u & 0 & 0 \\ 0 & \dot{\omega} & 0 & 0 & u\omega & \omega \end{bmatrix} \boldsymbol{\theta}, \tag{11}$$

where the vector of uncertainties was neglected. Regarding parametric uncertainties, the proposed control law is

$$\mathbf{v_r} = \hat{\mathbf{H}}(\dot{\mathbf{v}}'_\mathbf{d} + \mathbf{T}(\tilde{\mathbf{v}}')) + \hat{\mathbf{C}}\mathbf{v}'_\mathbf{d} + \hat{\mathbf{F}}\mathbf{v}'_\mathbf{d}, \tag{12}$$

where $\hat{\mathbf{H}}$, $\hat{\mathbf{C}}$, and $\hat{\mathbf{F}}$ are estimates of $\mathbf{H}$, $\mathbf{C}$, and $\mathbf{F}$, respectively, $\mathbf{T}(\tilde{\mathbf{v}}') = \begin{bmatrix} l_u & 0 \\ 0 & l_\omega \end{bmatrix} \begin{bmatrix} \tanh(\frac{k_u}{l_u} i\tilde{u}) \\ \tanh(\frac{k_\omega}{l_\omega}\tilde{\omega}) \end{bmatrix}$, $k_u > 0$ and $k_\omega > 0$ are gain constants, $l_u \in \mathbb{R}$ and $l_\omega \in \mathbb{R}$ are saturation constants, and $\tilde{\omega} = \omega_d - \omega$, $\tilde{u} = u_d - u$ are the current velocity errors. The term $\mathbf{T}(\tilde{\mathbf{v}}')$ provides a saturation in order to guarantee that the commands to be sent to the robot are always below the corresponding physical limits, considering that $\mathbf{v}'_\mathbf{d}$ and $\dot{\mathbf{v}}'_\mathbf{d}$ are bounded to appropriate values.

First, let us assume that there is no parameter estimation error. Using the Lyapunov candidate function $V = \frac{1}{2}\tilde{\mathbf{v}}'^{\mathbf{T}}\mathbf{H}\tilde{\mathbf{v}}' > 0$, and observing properties 3 and 5, one has $\dot{V} = -\tilde{\mathbf{v}}'^{\mathbf{T}}\mathbf{H}\mathbf{T}(\tilde{\mathbf{v}}') - \tilde{\mathbf{v}}'^{\mathbf{T}}\mathbf{F}\tilde{\mathbf{v}}' < 0$, which means that $\tilde{\mathbf{v}}' \in L_\infty$ and $\tilde{\mathbf{v}}' \to \mathbf{0}$ with $t \to \infty$ and, therefore, $\tilde{\mathbf{v}} \in L_\infty$ and $\tilde{\mathbf{v}} \to \mathbf{0}$ with $t \to \infty$.

Regarding the kinematic controller, we have shown in [21] that a sufficient condition for the asymptotic stability is

$$\|\tilde{\mathbf{h}}\| > \frac{\|\mathbf{A}\tilde{\mathbf{v}}\|}{min(k_x, k_y)}, \tag{13}$$

where $\mathbf{A} = \begin{bmatrix} \cos\psi & -a\sin\psi \\ \sin\psi & a\cos\psi \end{bmatrix}$. As $\tilde{\mathbf{v}}(t) \to \mathbf{0}$, the condition (13) is asymptotically verified for any value of $\tilde{\mathbf{h}}$. Consequently, the tracking control error $\tilde{\mathbf{h}}(t) \to \mathbf{0}$, thus accomplishing the control objective.

To continue to illustrate the application of the proposed model and its properties, let us consider the case in which the dynamic parameters are not correctly identified, or they change from task to task. In such a case, an updating control law is designed. To do so, let us rewrite the control law in its linear parametrization format

$$\mathbf{v_r} = \mathbf{G}\hat{\boldsymbol{\theta}} = \begin{bmatrix} \sigma_1 & 0 & -\omega_d\omega & u_d & 0 & 0 \\ 0 & \sigma_2 & (iu_d\omega - iu\omega_d) & 0 & u\omega_d & \omega_d \end{bmatrix}\hat{\boldsymbol{\theta}}, \tag{14}$$

where $\sigma_1 = \dot{u}_d + l_u \tanh(\frac{k_u}{l_u}\tilde{u})$, $\sigma_2 = \dot{\omega}_d + l_\omega \tanh(\frac{k_\omega}{l_\omega}\tilde{\omega})$. By defining the vector of parametric errors $\tilde{\boldsymbol{\theta}} = \hat{\boldsymbol{\theta}} - \boldsymbol{\theta}$, where $\hat{\boldsymbol{\theta}}$ is the vector of parameter estimates, Eq. 14 can be written as $\mathbf{v_r} = \mathbf{G}\boldsymbol{\theta} + \mathbf{G}\tilde{\boldsymbol{\theta}}$, or

$$\mathbf{v_r} = \mathbf{H}\boldsymbol{\sigma} + \mathbf{C}\mathbf{v}'_{\mathbf{d}} + \mathbf{F}\mathbf{v}'_{\mathbf{d}} + \mathbf{G}\tilde{\boldsymbol{\theta}}, \tag{15}$$

where $\boldsymbol{\sigma} = \dot{\mathbf{v}}'_{\mathbf{d}} + \mathbf{T}(\tilde{\mathbf{v}}')$. By recalling that $\tilde{\mathbf{v}}' = \mathbf{v}'_{\mathbf{d}} - \mathbf{v}'$, one can conclude that $\dot{\mathbf{v}}'_{\mathbf{d}} = \dot{\tilde{\mathbf{v}}}' + \dot{\mathbf{v}}'$. Then, $\boldsymbol{\sigma} = \dot{\tilde{\mathbf{v}}}' + \mathbf{T}(\tilde{\mathbf{v}}') + \dot{\mathbf{v}}'$. Substituting this term in Eq. 15, the closed loop equation is

$$-\mathbf{G}\tilde{\boldsymbol{\theta}} = \mathbf{H}(\dot{\tilde{\mathbf{v}}}' + \mathbf{T}(\tilde{\mathbf{v}}')) + \mathbf{C}\tilde{\mathbf{v}}' + \mathbf{F}\tilde{\mathbf{v}}'. \tag{16}$$

Let us consider $V = \frac{1}{2}\tilde{\mathbf{v}}'^{\mathbf{T}}\mathbf{H}\tilde{\mathbf{v}}' + \frac{1}{2}\tilde{\boldsymbol{\theta}}^{\mathbf{T}}\boldsymbol{\gamma}^{-1}\tilde{\boldsymbol{\theta}} > 0$ as the Lyapunov candidate function. Using Eq. 16, it results that

$$\dot{V} = -\tilde{\mathbf{v}}'^{\mathbf{T}}(\mathbf{G}\tilde{\boldsymbol{\theta}} + \mathbf{C}\tilde{\mathbf{v}}' + \mathbf{F}\tilde{\mathbf{v}}') - \tilde{\mathbf{v}}'^{\mathbf{T}}\mathbf{H}\mathbf{T}(\tilde{\mathbf{v}}') + \tilde{\boldsymbol{\theta}}^{\mathbf{T}}\boldsymbol{\gamma}^{-1}\dot{\tilde{\boldsymbol{\theta}}}. \tag{17}$$

where $\boldsymbol{\gamma}^{-1} \in \mathbb{R}^{6\times 6}$ is a diagonal positive definite matrix. For now, let us consider that there is no parameter changing during the accomplishment of the task, i.e., $\dot{\boldsymbol{\theta}} = \mathbf{0}$ and $\dot{\hat{\boldsymbol{\theta}}} = \dot{\tilde{\boldsymbol{\theta}}}$.

By choosing the updating law as

$$\dot{\hat{\boldsymbol{\theta}}} = \boldsymbol{\gamma}\mathbf{G}^{\mathbf{T}}\tilde{\mathbf{v}}', \tag{18}$$

and using property 5 (skew symmetry of $\mathbf{C}$), Eq. 17 results in

$$\dot{V} = -\tilde{\mathbf{v}}'^{\mathbf{T}}\mathbf{F}\tilde{\mathbf{v}}' - \tilde{\mathbf{v}}'^{\mathbf{T}}\mathbf{H}\mathbf{T}(\tilde{\mathbf{v}}') \leq 0,$$

which is semi-definite negative. Hence, it can be concluded that $\tilde{\boldsymbol{\theta}} \in L_\infty$, $\tilde{\mathbf{v}}' \in L_\infty$ and, therefore, $\tilde{\mathbf{v}} \in L_\infty$. By integrating $\dot{V}$ it results that

$$V(T) - V(0) = -\int_0^T \tilde{\mathbf{v}}'^{\mathbf{T}}\mathbf{H}\mathbf{T}(\tilde{\mathbf{v}}')dt - \int_0^T \tilde{\mathbf{v}}'^{\mathbf{T}}\mathbf{F}\tilde{\mathbf{v}}'dt.$$

If the term $V(T)$ is dropped, the previous equation can be written as the inequality

$$\int_0^T \|\tilde{\mathbf{v}}'\|^2 dt \leq \frac{V(0) - \alpha}{\lambda_{min}(\mathbf{F})} \Rightarrow \int_0^\infty \|\tilde{\mathbf{v}}'\|^2 dt \leq \frac{V(0) - \alpha}{\lambda_{min}(\mathbf{F})}, \tag{19}$$

where $\alpha = \int_0^\infty \tilde{\mathbf{v}}'^{\mathbf{T}}\mathbf{H}\mathbf{T}(\tilde{\mathbf{v}}')dt$.

The above inequality is valid for any value of T. Thus, it can be concluded that $\tilde{\mathbf{v}}'$ is a square integrable signal, i.e., $\tilde{\mathbf{v}}' \in L_2$, and hence $\tilde{\mathbf{v}} \in L_2$. Assuming that $\mathbf{v}'_{\mathbf{d}}$ is bounded, as $\tilde{\mathbf{v}}' = \mathbf{v}'_{\mathbf{d}} - \mathbf{v}'$ and $\tilde{\mathbf{v}}'$ is bounded, one can conclude that $\mathbf{v}'$ is also bounded. Thus, $\mathbf{C}(\mathbf{v})$ and $\mathbf{F}(\mathbf{v})$ are bounded. Considering that $\dot{\mathbf{v}}'_{\mathbf{d}}$ is bounded it can be concluded that $\mathbf{G}$ is also bounded. Property 4 states that $\mathbf{H}$ is constant, and it is known that $\tilde{\boldsymbol{\theta}}$, $\tilde{\mathbf{v}}'$ and $\mathbf{T}(\tilde{\mathbf{v}}')$ are bounded. So, from Eq. 16 it can be noticed that $\dot{\tilde{\mathbf{v}}}'$ is bounded, i.e., $\dot{\tilde{\mathbf{v}}}' \in L_\infty$. As $\dot{\tilde{\mathbf{v}}}' \in L_\infty$ and $\tilde{\mathbf{v}}' \in L_2$, Barbalat lemma guarantees that $\tilde{\mathbf{v}}'(t) \to \mathbf{0}$ with $t \to \infty$. Therefore, $\tilde{\mathbf{v}}(t) \to \mathbf{0}$ with $t \to \infty$, which proves that the control objective is accomplished.

The parameter updating law (18) works as an integrator and can cause robustness problems in case of measurement errors, noise or disturbances. A possible way of preventing parameter drifting is to turn parameter updating off when the error value is smaller than a certain bound, as illustrated in [20]. Another known way of preventing parameter drifting is to change the parameter updating law by introducing a Leakage term, or a σ-modification [4, 15]. By including such term, the robust updating law

$$\dot{\hat{\boldsymbol{\theta}}} = \boldsymbol{\gamma}\mathbf{G}^{\mathbf{T}}\tilde{\mathbf{v}}' - \boldsymbol{\gamma}\Gamma\hat{\boldsymbol{\theta}} \tag{20}$$

is obtained, where $\boldsymbol{\Gamma} \in \mathbb{R}^{6\times 6}$ is a diagonal positive gain matrix.

By using the same Lyapunov function as before, and applying a technique similar to the one we have presented in [21], it is possible to show that the stability of the equilibrium is guaranteed if the disturbance is limited. Finally, it is also possible to prove that the tracking error $\tilde{\mathbf{h}}$ is ultimately bounded.

Because we cannot guarantee that the control signals are sufficiently rich, it should be pointed out that the proposed controller does not guarantee that $\tilde{\boldsymbol{\theta}} \to \mathbf{0}$ when $t \to \infty$. In other words, parameter estimates might converge to values that do not correspond to the physical parameters. Actually, this does not represent a problem because it is not required that $\tilde{\boldsymbol{\theta}} \to \mathbf{0}$ in order to make $\tilde{\mathbf{v}}$ converge to a bounded value.

This concludes our example of application of the proposed model and its properties on the design and stability analysis of a dynamic compensation controller.

5 Results and Discussion

To illustrate the application and relevance of the dynamic model, we are going to compare the simulation results of four cases. In the first case, only the robot kinematic model is considered and the robot is directly controlled by the kinematic controller. This is the classical situation in which the dynamics of the mobile robot is not considered in the simulation. In the other cases, the complete dynamic model of the Pioneer 3-DX with LASER is considered, including speed and acceleration limitations. In the second simulation, only the kinematic controller is used. In the third and fourth simulations, the adaptive dynamic compensation controller is also used. The difference is that in the third simulation the parameter estimates are exactly equal to the robot parameters (ideal case), while the fourth simulation deals with the more realistic case in which the initial parameter estimates are different from the robot parameters.

We used MATLAB/Simulink® to implement the control structure shown on Fig. 2 using the control laws given by Eqs. 10 and 12, with the robust updating law given by Eq. 20. In all simulations the robot starts at position $(0.2, 0.0)$ m with orientation 0 degrees, and should follow an 8-shape trajectory starting at $(0.0, 0.0)$ m. The trajectory to be followed by the robot is represented by a sequence of desired positions $\mathbf{h_d}$ and velocities $\dot{\mathbf{h}}_\mathbf{d}$, both varying in time.

The following parameters were used in all simulations: fixed sample time of 0.1 s (this is the sample time of the Pioneer 3-DX); controller gains $k_x = 0.1$, $k_y = 0.1$, $k_u = 4$, $k_w = 4$; saturation constants $l_x = 0.1$, $l_y = 0.1$, $l_u = 1$, $l_w = 1$; adaptation gains $\boldsymbol{\gamma} = diag(1.7, 1.1, 0.5, 0.3, 0.01, 0.5)$; and sigma modification $\boldsymbol{\Gamma} = diag(0.0005, 0.001, 0.001, 0.00006, 0.001, 0.001)$.

Figure 3a and b show the path followed by the robot and the evolution of the distance error during the first simulation. The distance error is defined as the instantaneous distance between the reference position $\mathbf{h_d}$ and the robot position $\mathbf{h}$. It can be noticed that the distance error starts in 0.2 m, as expected, and decreases to zero as the simulation progresses. The trajectory to be followed by the robot is shown in Fig. 4a in the form of desired positions along time, decomposed in X and Y axes. The same figure also presents the actual X and Y values of the robot position. One should notice that the desired X and Y positions vary in time, which forces the robot to change its linear and angular velocities along the path as illustrated in Fig. 4b. Because the robot dynamics is neglected in this case, a perfect velocity tracking is implicitly assumed, i.e., $\mathbf{v_d} = \mathbf{v}$. Therefore, in Fig. 4b is not possible to see the difference between reference and actual velocities. This is reflected in the evolution of the distance error, which remains equal to zero while the robot is following the trajectory.

The perfect velocity tracking assumption does not result in significant errors in some cases. But, in other situations the consideration of the dynamic model is very important. To illustrate this, in the second simulation we include the dynamic model into the same system and repeat the experiment using the same kinematic controller as in the first simulation. Now, the desired velocities generated by the kinematic controller are sent to the robot model that includes its dynamics ($\mathbf{v_d} = \mathbf{v_r}$).

Figure 5a and b show the path followed by the robot and the evolution of the distance error during the second simulation. One should immediately notice the difference in performance when compared to the first simulation. Now, the distance error does not decrease to zero as the simulation progresses. Instead, it oscillates around 0.1 m and the path followed by the robot is distorted. Figure 6a shows the desired and actual X

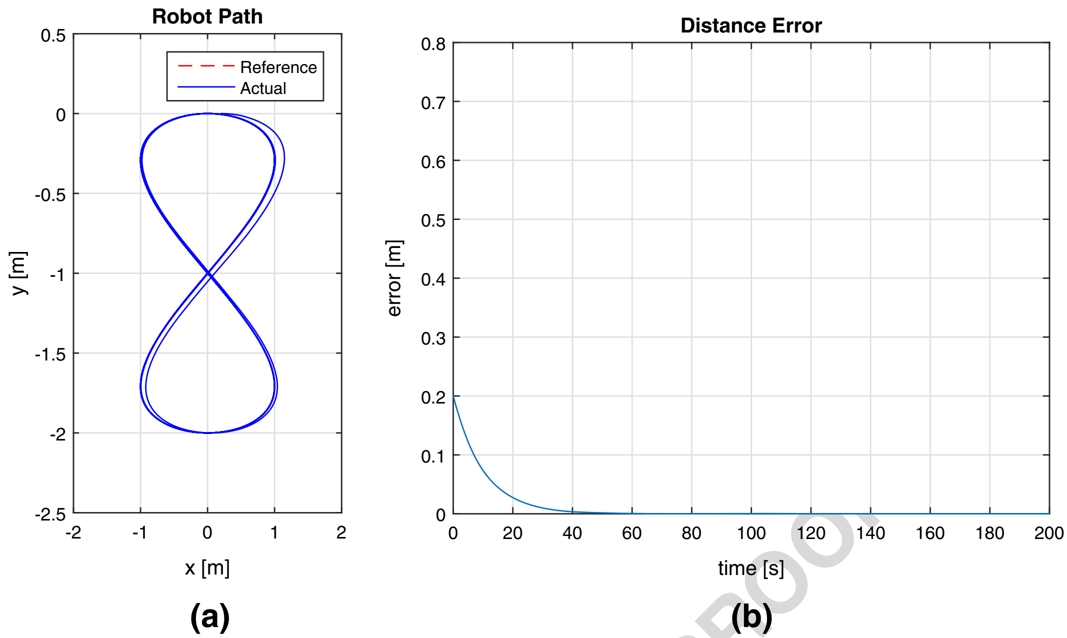

Fig. 3 Kinematic controller and kinematic model only: **a** Robot path; **b** Evolution of distance error

and Y positions, where it can be seen that the robot is always behind the desired position. Figure 6b presents the reference and actual values of linear and angular velocities. Now, it is clear that the actual robot velocities are not exactly equal to the desired ones generated by the kinematic controller. This is the reason why the tracking error never drops to zero and the path followed by the robot is not equal to the desired one.

The results of the first and second simulations illustrate that considering the dynamic model is very important for the evaluation of controller performance under simulation. If we were to tune the controller based on the first simulation, the real world performance of the kinematic controller could be non satisfactory. It is important to mention that an increase in controller gains k_x and k_y would result in better

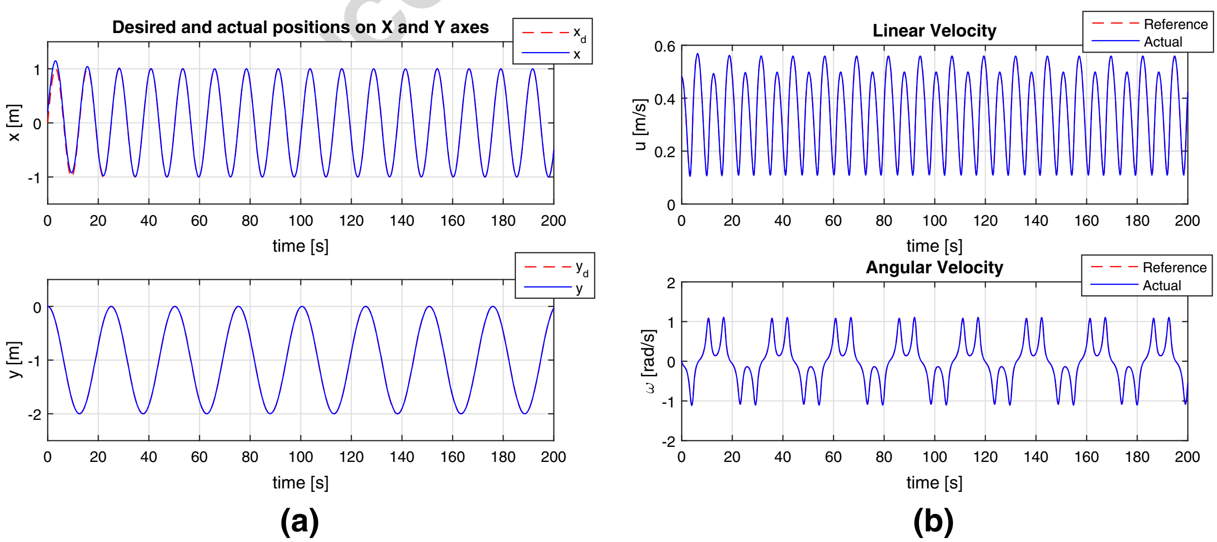

Fig. 4 Kinematic controller and kinematic model only: **a** desired and actual positions; **b** linear and angular velocities

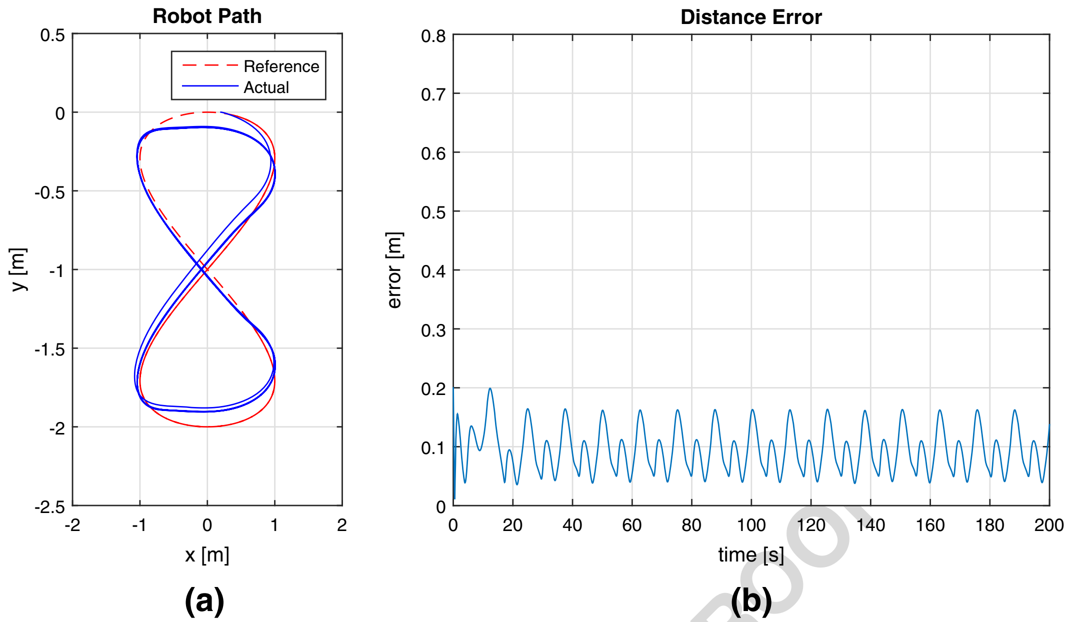

Fig. 5 Kinematic controller and dynamic model: **a** Robot path; **b** Evolution of distance error

performance (smaller tracking error). Nevertheless, we kept the same values of controller gains during all four simulations to be able to compare the results.

Now, let us analyze the system performance with the addition of the dynamic compensation controller. In this third simulation, we use the exact values of the robot parameters as estimates on the dynamic controller (ideal case of dynamic compensation). Figure 7a and b show the path followed by the robot and the evolution of the distance error, while Fig. 8a and b show the desired and actual X and Y positions, and the robot linear and angular velocities, respectively, during the third simulation. By comparing this results with the ones from the first simulation (Figs. 3a, b, 4a and b) it can be seen that the system performance is very similar. This means that the

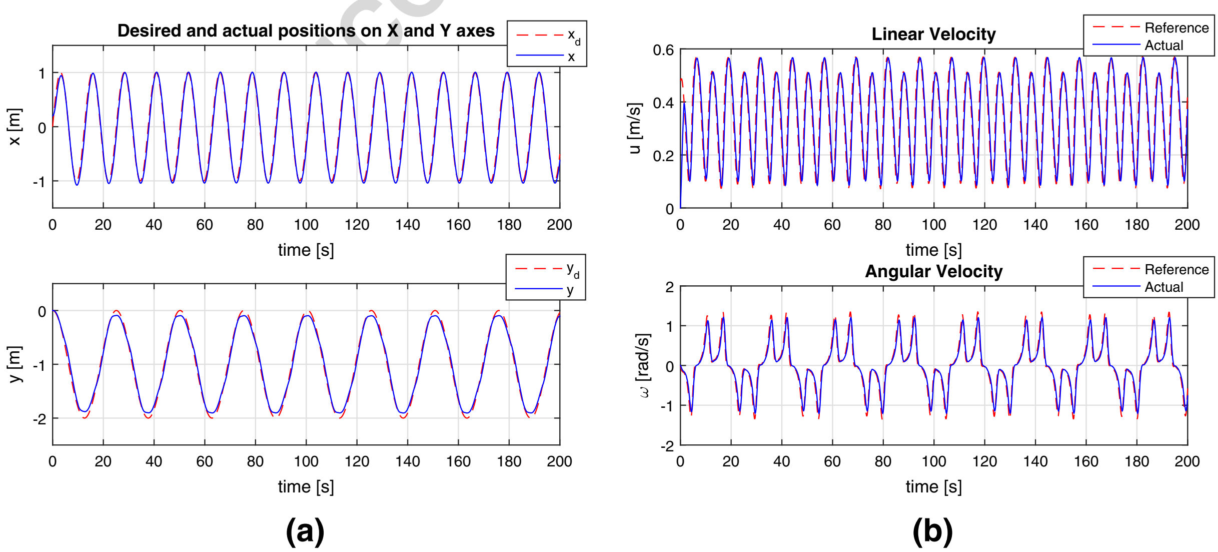

Fig. 6 Kinematic controller and dynamic model: **a** desired and actual positions; **b** linear and angular velocities

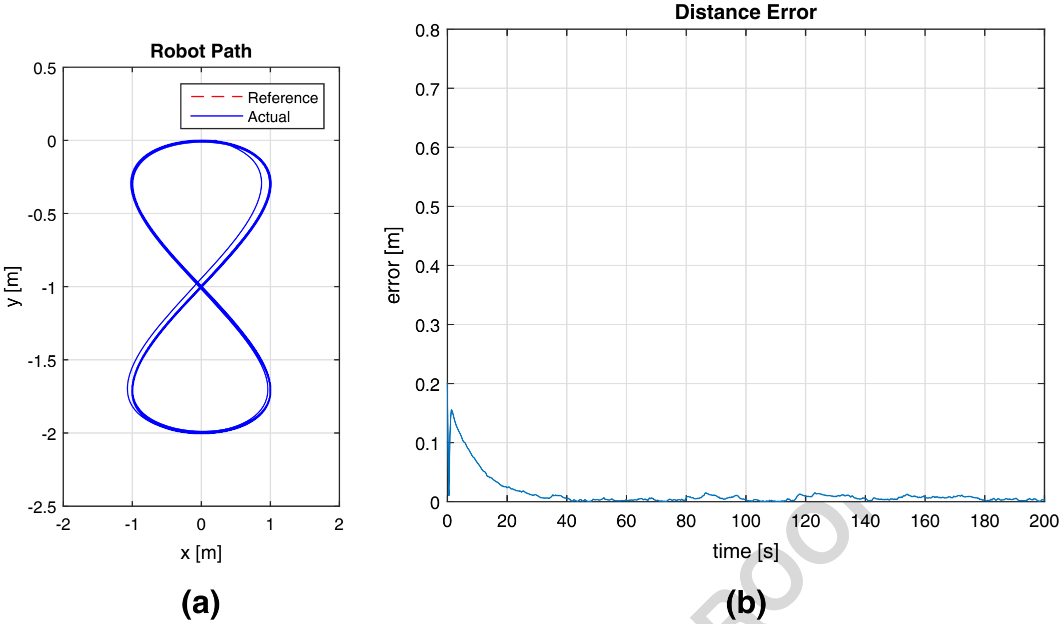

Fig. 7 Perfect dynamic compensation: **a** Robot path; **b** Evolution of distance error

dynamic compensation controller is able to cancel out the effects of the robot dynamics almost perfectly. The cancellation of the dynamic effects is not perfect because, in order to have a more realistic simulation, we have included white noise in the values of position and velocities that are fed back to the controllers.

The fourth simulation repeats the third one with the same conditions, except that the initial parameter

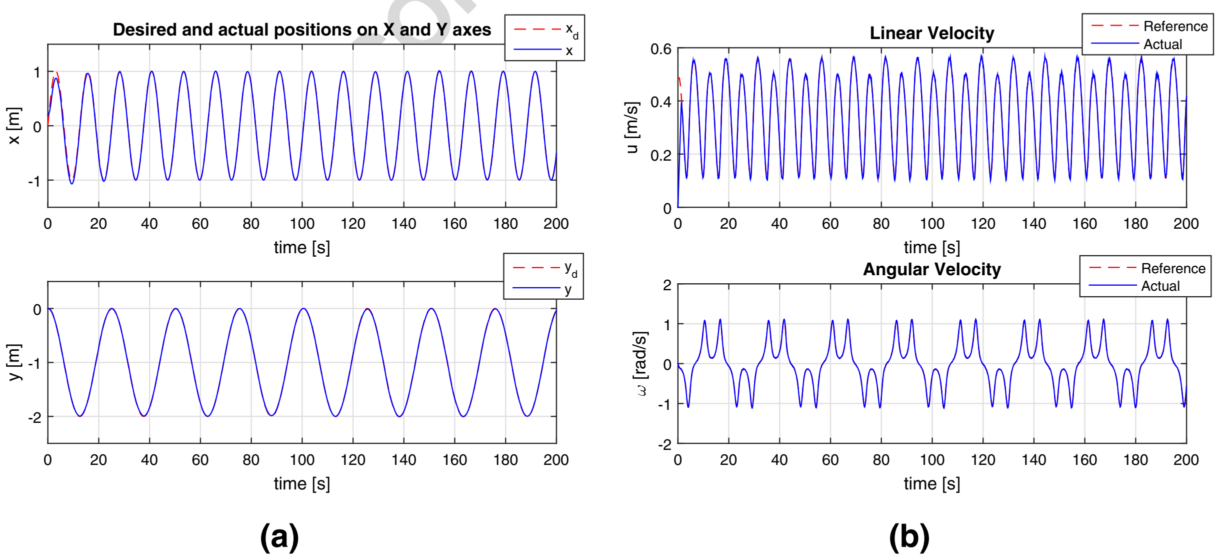

Fig. 8 Perfect dynamic compensation: **a** desired and actual positions; **b** linear and angular velocities

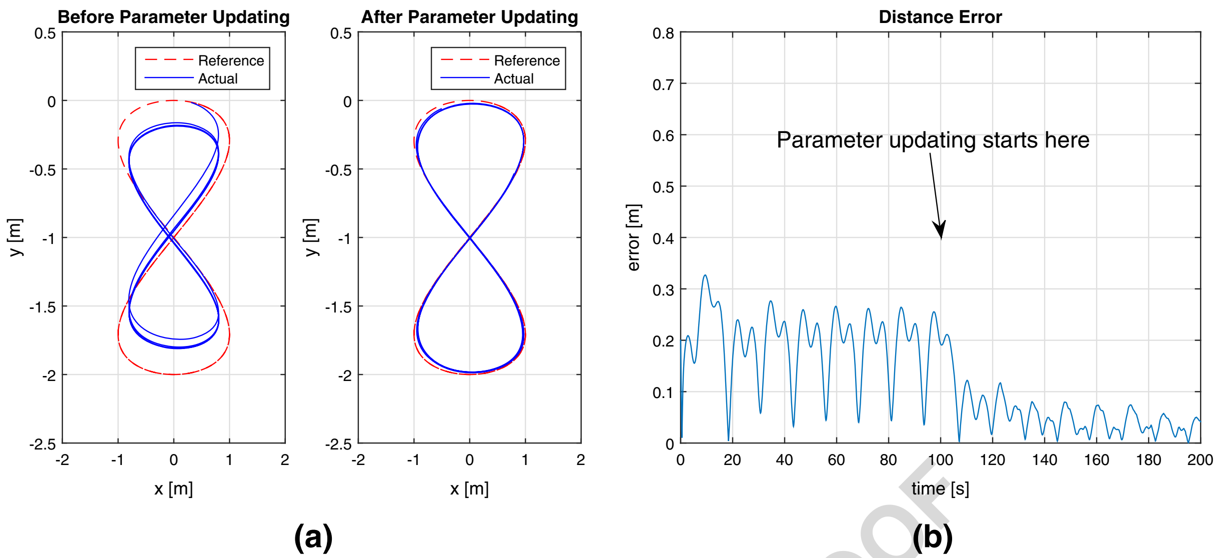

Fig. 9 Adaptive dynamic compensation: **a** Robot path before and after parameter updating; **b** Evolution of distance error

estimates used in the controller were different from the real robot parameters (about 30 % difference). The initial values of parameter estimates used in the fourth simulation are: $\hat{\boldsymbol{\theta}} = [0.1736\ 0.1673\ -0.0003\ 0.6643\ 0.0018\ 0.7179]$. The simulation begins with no parameter updating, which starts only at $t = 100$ s and remains active until the simulation stops.

Figure 9a and b illustrate, respectively, the robot path before and after the parameter updating activation, and the evolution of the distance error during the simulation. Notice that the distance error oscillates around 0.2 m until the activation of the parameter updating at $t = 100$ s. Then, the error is reduced, reaching a value smaller than 0.05 m at $t = 200$ s. Figure 10a and b present the evolution of the the desired and actual X and Y positions, and the robot linear and angular velocities, respectively. Notice the reduction in velocity error after the start of parameter

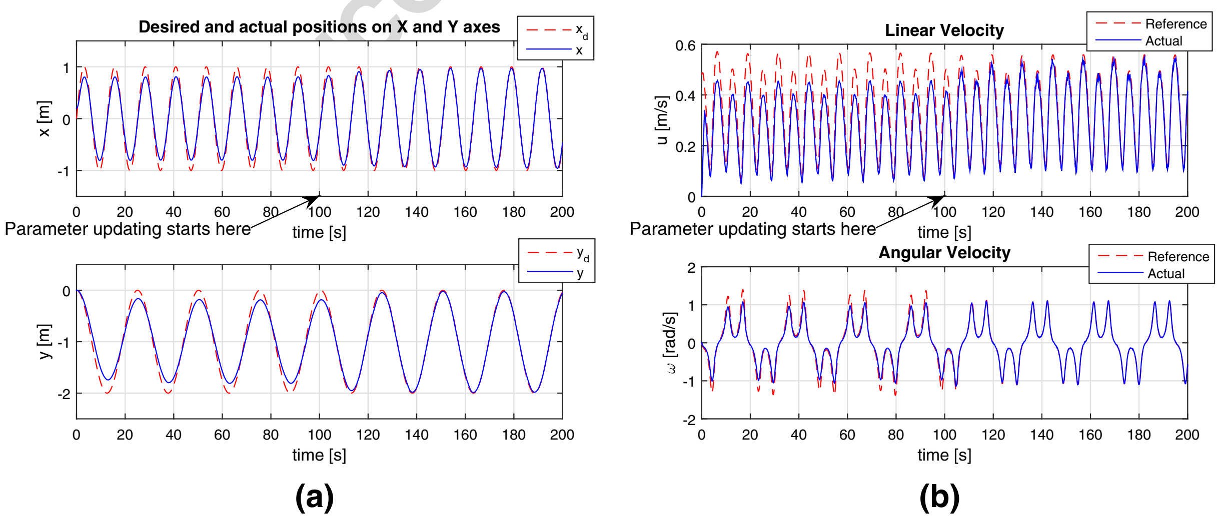

Fig. 10 Adaptive dynamic compensation: **a** desired and actual positions; **b** linear and angular velocities

updating. All figures clearly show a change in performance after the start of parameter update, which indicates the importance of considering the dynamic model in the design of robot motion controllers.

We have also evaluated the system performance for different values of controller gains k_x and k_y. To do that, several $T = 250$ s simulations were executed, in which the robot should follow an 8-shape trajectory. For each simulation we calculted the IAE performance index, where $IAE = \int_0^T |E(t)|dt$, $E(t) = \sqrt{\tilde{x}^2 + \tilde{y}^2}$ is the instantaneous distance error, and T is the simulation period. In each simulation, the kinematic controller gains ($k_x = k_y$) were set to different values ranging from 0.5 to 35, while all of the dynamic compensation controller gains were kept constant. Simulations were performed for the following cases:

(a) only the kinematic controller was enabled, i.e., the robot receives the reference velocities $\mathbf{v_d}$ directly from the kinematic controller;
(b) the dynamic compensation was activated with wrong parameter estimates (10 %) and parameter updating was disabled;
(c) the dynamic compensation was activated starting with wrong parameter estimates (10 %) and parameter updating was enabled since $t = 0$ s; and
(d) the dynamic compensation was activated with exact parameter estimates (ideal case) without parameter updating.

Figure 11 shows the IAE values obtained via several simulations for each of the above mentioned cases. For the case (a), it can be seen from Fig. 11 that the IAE value is higher than 8 for $k_x = k_y = 1$, and gets smaller as the value of the controller gains increases. For this case, better performance is obtained when $k_x = k_y = 23$, when IAE reaches its minimum value of 1.24. The same simulations were repeated for the cases (b), (c), and (d) with the adaptive dynamic compensation activated. Figure 11 shows that the inclusion of the adaptive compensation controller results on smaller IAE values, thus improving system performance for any value of $k_x = k_y$. As expected, the error is smaller for the ideal case (d), which illustrates the importance of the consideration of the dynamic model on the design of the robot controller. Even under the unfavorable conditions correspondent to cases (b) and (c), the resulting IAE values are smaller when the dynamic compensation controller is activated.

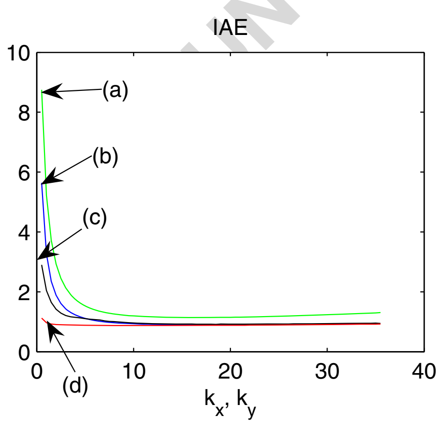

Fig. 11 IAE for 250 s simulations for the cases (a-d) (see text)

Finally, we have also tested the controllers on a real robot, namely a Pioneer 3-DX robot, using the control laws in Eqs. 10 and 12, with the robust updating law given in Eq. 20. The experiment was executed under similar conditions that were used in the fourth simulation: the robot starts at (0.2, 0.0) m, and should follow an 8-shape trajectory starting at (0.0, 0.0) m. Its linear velocity varies from 0.2 m/s to 0.4 m/s, and its angular velocity varies from −0.8 rad/s to 0.8 rad/s. The initial parameter estimates used in the controller were different from the real robot parameters of about 20 %. The experiment begins with no parameter updating, which, in this case, starts at $t = 30$ s. Robot trajectory was recovered through its odometry. The effectiveness of the adaptive controller was evaluated by calculating the value of IAE for a period of 15 s before and after parameter updating. Between $t = 15$ s and $t = 30$ s the value of IAE was 14.38. On the other hand, the value of IAE calculated between $t = 45$ s and $t = 60$ s, 15 s after the activation of parameter updating, was 6.55, about 50 % smaller. The experiment was repeated under the same conditions, but using only the kinematic controller (10). For this case, the value of IAE calculated between $t = 45$ s and $t = 60$ s was 9.06. This result reinforces the effectiveness of the use of our proposed dynamic model in the design of a dynamic compensation scheme when compared to control systems that consider only the robot kinematic model.

6 Conclusion

We have presented a formulation and the mathematical properties of a velocity-based dynamic model, which are useful on the design and stability analysis of mobile robot controllers. Regarding the model properties, it is interesting to notice that $(\dot{\mathbf{H}} - 2\mathbf{C})$ is skew symmetric because $\mathbf{H}$ is constant (hence $\dot{\mathbf{H}} = \mathbf{0}$), and $\mathbf{C}$ is skew symmetric. Also, the mathematical structure we propose (6) is similar to the classical torque-based model that describes the dynamics of mobile robots and manipulators. Therefore, existent strategies for torque-based controller design [12–14, 18, 29] can be adapted to design controllers for mobile robots using the proposed model.

As any other dynamic model, our model provides more accurate simulation results when compared with models that are based only on the kinematics of the robot. Therefore, it can be used to obtain more realistic results on controller tuning under simulation, providing a more precise evaluation of real robot behaviour. Moreover, it can be easily integrated into simulation models that have been built for the differential-drive kinematics, as we shown in Section 5. For example, our model can be used in connection with kinematic controllers that were designed for commercial mobile robots, like the Pioneer robots from Adept-Mobile Robots, the robuLAB-10 from Robosoft Inc. and the Khepera robots from K-Team Corporation. This integration requires no change on the original controller equations since it accepts the same velocity commands as commercial robots. To illustrate this concept, we have built simulation blocks for MATLAB/Simulink® which include the differential-drive kinematics and dynamics, a kinematic controller and two adaptive dynamic compensation controllers. The simulation blocks are ready-to-use and are available for download [19]. The kinematic and dynamic model blocks were also included in version 9.10 of Peter Corke's Robotics Toolbox for MATLAB® [6].

To sum up, we have proposed a new approach to write the velocity-based dynamic model for differential drive mobile robots, the study of its mathematical properties and presented the design of an adaptive dynamic compensation controller as an example application. These are the main contributions of the present paper.

Acknowledgements The authors thank CAPES (Brazil) and SPU (Argentina) for funding the partnership between the Federal University of Espirito Santo (UFES), Brazil, and the National University of San Juan (UNSJ), Argentina. They also thank the Federal Institute of Education, Science and Technology of Espirito Santo (IFES) for the financial support to the English revision of this text.

References

1. Andaluz, V.H., Canseco, P., Varela, J., Ortiz, J.S., Pérez, M.G., Roberti, F., Carelli, R.: Robust control with dynamic compensation for human-wheelchair system. In: Intelligent Robotics and Applications, pp. 376–389. Springer (2014)
2. Antonini, P., Ippoliti, G., Longhi, S.: Learning control of mobile robots using a multiprocessor system. Control. Eng. Pract. (14):1279–1295 (2006)
3. Birk, A., Kenn, H.: Roboguard, a teleoperated mobile security robot. Control. Eng. Pract. (10) 1259–1264 (2002)
4. Boyd, S., Sastry, S.: Adaptive control: stability, convergence, and robustness. Prentice Hall, USA (1989)
5. Chen, C., Li, T., Yeh, Y., Chang, C.: Design and implementation of an adaptive sliding-mode dynamic controller for wheeled mobile robots. Mechatronics **19**(2), 156–166 (2009)
6. Corke, P.: Robotics, Vision and Control: Fundamental Algorithms in MATLAB, vol. 73. Springer, Berlin (2011)
7. Das, T., Kar, I.: Design and implementation of an adaptive fuzzy logic-based controller for wheeled mobile robots. IEEE Trans. Control Syst. Technol. **14**(3), 501–510 (2006)
8. De La Cruz, C., Carelli, R.: Dynamic model based formation control and obstacle avoidance of multi-robot systems. Robotica **26**(03), 345–356 (2008)
9. De La Cruz, C., Celeste, W., Bastos-Filho, T.: A robust navigation system for robotic wheelchairs. Control. Eng. Pract. **19**(6), 575–590 (2011)
10. Do, K.: Bounded controllers for global path tracking control of unicycle-type mobile robots. Robot. Auton. Syst. (2013)
11. Fierro, R., Lewis, F.L.: Control of a nonholonomic mobile robot: Backstepping kinematics into dynamics. J. Robot. Syst. **14**(3), 149–163 (1997)
12. He, W., Chen, Y., Yin, Z.: Adaptive neural network control of an uncertain robot with full-state constraints. IEEE Trans. Syst. Man Cybern. Syst. **46**(3), 620–629 (2015)
13. He, W., David, A.O., Yin, Z., Sun, C.: Neural network control of a robotic manipulator with input deadzone and output constraint. IEEE Trans. Cybern. PP(99) (2015)
14. He, W., Dong, Y., Sun, C.: Adaptive neural impedance control of a robotic manipulator with input saturation. IEEE Trans. Syst. Man Cybern. Syst. **46**(3), 334–344 (2015)
15. Kaufman, H., Sobel, K.: Direct Adaptive Control Algorithms: Theory and Applications, pp. 182–184 (1998)

16. Lapierre, L., Zapata, R., Lepinay, P.: Combined path-following and obstacle avoidance control of a wheeled robot. Int. J. Robot. Res. **26**(4), 361–375 (2007)
17. Laut, J.: A dynamic parameter identification method for migrating control strategies between heterogeneous wheeled mobile robots. Ph.D. thesis, Worcester Polytechnic Institute (2011)
18. Lewis, F.L., Dawson, D.M., Abdallah, C.T.: Robot Manipulator Control: Theory and Practice. CRC Press, Boca Raton (2003)
19. Martins, F.: Velocity-based dynamic model and adaptive controller for differential steered mobile robot. Available at http://www.mathworks.com/matlabcentral/fileexchange/44850 (2013)
20. Martins, F., Celeste, W., Carelli, R., Sarcinelli-Filho, M., Bastos-Filho, T.: Kinematic and adaptive dynamic trajectory tracking controller for mobile robots. In: 3rd International Conference on Advances in Vehicle Control and Safety - AVCS07. Buenos Aires, Argentina (2007)
21. Martins, F., Celeste, W., Carelli, R., Sarcinelli-Filho, M., Bastos-Filho, T.: An adaptive dynamic controller for autonomous mobile robot trajectory tracking. Control Eng. Pract. **16**, 1354–1363 (2008). doi:10.1016/j.conengprac.2008.03.004
22. Morin, P., Samson, C.: Motion control of wheeled mobile robots. In: Springer Handbook of Robotics, pp. 799–826. Springer (2008)
23. Onat, A., Ozkan, M.: Dynamic adaptive trajectory tracking control of nonholonomic mobile robots using multiple models approach. Adv. Robot. **29**(14), 913–928 (2015)
24. Prassler, E., Ritter, A., Schaeffer, C., Fiorini, P.: A short history of cleaning robots. Auton. Robot. **9**(3), 211–226 (2000)
25. Rossomando, F.G., Soria, C., Carelli, R.: Adaptive neural sliding mode compensator for a class of nonlinear systems with unmodeled uncertainties. Eng. Appl. Artif. Intell. **26**(10), 2251–2259 (2013)
26. Schaft, A.J.v.d.: L2-Gain and Passivity Techniques in Nonlinear Control. Springer, Berlin (1999)
27. Shojaei, K., Mohammad Shahri, A., Tarakameh, A.: Adaptive feedback linearizing control of nonholonomic wheeled mobile robots in presence of parametric and nonparametric uncertainties. Robot. Comput. Integr. Manuf. **27**(1), 194–204 (2011)
28. Siegwart, R., Nourbakhsh, I., Scaramuzza, D.: Introduction to Autonomous Mobile Robots, 2nd edn. MIT Press, Cambridge (2011)
29. Spong, M.W., Hutchinson, S., Vidyasagar, M.: Robot Modeling and Control, vol. 3. Wiley, New York (2006)
30. Stouten, B., de Graaf, A.: Cooperative transportation of a large object-development of an industrial application. In: IEEE International Conference on Robotics and Automation, vol. 3, pp. 2450–2455 (2004)
31. Utstumo, T., Berge, T.W., Gravdahl, J.T.: Non-linear model predictive control for constrained robot navigation in row crops. In: IEEE International Conference on Industrial Technology (ICIT 2015) (2015)
32. Wang, K.: Near-optimal tracking control of a nonholonomic mobile robot with uncertainties. Int. J. Adv. Robot. Syst. 9(66) (2012)

AUTHOR QUERIES

AUTHOR PLEASE ANSWER ALL QUERIES:

Q1. Author biography are required. Please provide.
Q2. Please check affiliations if presented correctly.
Q3. Please check corresponding author email address if correct.
Q4. Please provide volume no. in reference [3].
Q5. Please provide volume and pages in reference [10].
Q6. Please provide pages in reference [13, 32].
Q7. Please check initials in reference [26] if correct.